ANALYTICAL AND NUMERICAL STUDIES OF

EFFECTIVE MEDIUM MIXING PROBLEMS IN ELECTROMAGNETICS

An Undergraduate Research Scholars Thesis

by

NICHOLAS N. MAI

Submitted to the Office of Honors and Undergraduate Research
Texas A&M University
in partial fulfillment of the requirements for the designation as

UNDERGRADUATE RESEARCH SCHOLAR

Approved by
Research Advisor: Dr. Gregory Huff

May 2013

Major: Electrical Engineering

TABLE OF CONTENTS

Page

TABLE OF CONTENTS……1

ABSTRACT……...……...2

DEDICATION……..……4

ACKNOWLEDGEMENTS……5

NOMENCLATURE……...…….7

CHAPTER

I INTRODUCTION……...8

II THEORETICAL BACKGROUND……...11

Review of the theory of electromagnetics and dielectric materials……...11
Classical mixing theory…….....13

III ANALYTICAL APPROACH……...15

Single layered dielectric inclusions……...15
Two layered dielectric inclusions……..18
Field perturbation analysis……21

IV NUMERICAL SIMULATIONS……23

COMSOL simulation setup and governing equations……...26
CST Microwave Studio setup……....28
Results from COMSOL simulations……..31

V CONCLUSIONS AND FUTURE WORK……36

REFERENCES……..37

ABSTRACT

Analytical and Numerical Studies of
Effective Medium Mixing Problems in Electromagnetics (May 2013)

Nicholas Mai
Department of
Electrical & Computer Engineering
Texas A&M University

Research Advisor: Dr. Gregory Huff
Department of
Electrical & Computer Engineering

Electromagnetically Functionalized Colloidal Dispersions (EFCDs) have been utilized in several applications in electromagnetics such as reconfigurable antennas. The colloidal dispersions vary the electrical properties depending on the volume fraction relative to the background fluid. The classical Maxwell-Garnett mixing formulas are an effective medium theory that provides a capable framework for approximating the effective electromagnetic properties of these EFCD mixtures. However, the theory only accounts for first-order interactions of the mixed inclusions at lower volume fractions, so deviations from the theory occur at high volume fraction. Thus, accurately modeling and predicting the effective permittivity of a mixture is still a problem to be solved.

This thesis presents an analytical and numerical study of the effective properties for EFCDs. An analysis in the quasi-static regime leads to the development of a new model that adds higher-order interactions to the Maxwell Garnett theory. Additionally, finite-element simulations using both COMSOL and Computer Simulation Technology Microwave Studio are performed to compute the effective medium permittivity. Several particle distributions are analyzed using a

frequency dependent potential boundary condition to validate the analytical model as well as study the effects of percolation at high volume fractions. These results will show that the Maxwell-Garnett theory clearly breaks down at higher volume fractions.

DEDICATION

To my ALL of family and friends.

ACKNOWLEDGEMENTS

I would like to thank my research advisor, Dr. Gregory Huff, for his guidance and support throughout the course of this most interesting project. My work would not have been possible if not for the numerous resources he provided.

I am also deeply appreciative towards all of the members of the Huff Research Group. They treated me as an equal despite all being much wiser and more experienced in the field of electromagnetics.

In particular, I thank Franklin Drummond for the spending the countless hours (in particular, Saturday March 23, 2013) helping me analyze and model this problem; without his assistance and previous work, much of this thesis would not have been possible. I thank Michael Kelley for providing much needed social support and mutual commiseration. I thank Kristopher Buchanan for letting me use his own office space to do my research and work in the laboratory. I thank Nicholas Brennan for allowing a second Nick in the lab and helping me finish computer related tasks. I thank Joel D. Barrera for his assistance in handling the finer details of modeling RF problems. I think David Rolando for being my office neighbor and listening to my many mathematical ramblings.

I could not have finished this work without the support of my friends at this university, for they never let me forget the importance of all work and no play.

Finally, my s would not have been possible if not for the sacrifices my family made to let me come to this university.

NOMENCLATURE

AC	Alternating Current
BCC	Body-Centered Cubic
BSTO	Barium Strontium Titanate
CST	Computer Simulation Technology
CST-MWS	Computer Simulation Technology – Microwave Studio
EFCD	Electromagnetically Functionalized Colloidal Dispersions
EMT	Effective Medium Theory
EQS	Electro Quasi-Static
FCC	Face-Centered Cubic
TE	Transverse Electric
VSWR	Voltage Standing-Wave Ratio

CHAPTER I

INTRODUCTION

The problem of characterizing a material's electrical properties is extremely important to the field of electromagnetics. The design of many high frequency components such as antennas and transmission lines requires the knowledge of how electromagnetic fields affect and are affected by a medium. For example, the attenuation and propagation constants in any transmission line are directly related to the square root of the line's dielectric permittivity [1].

In the Texas A&M University Electromagnetics and Microwaves Laboratory, electrically reconfigurable antennas are one of the main research topics. Figure 1 shows a microstrip patch antenna with embedded fluid channels (capillaries) running through the center of the substrate [2]. During operation, electrically active fluids are passed through these channels, altering the net effective permittivity of the substrate under the patch. In response, the resonant frequency and voltage-standing wave ratio (VSWR) bandwidth decrease depending on the effective dielectric permittivity of the fluid.

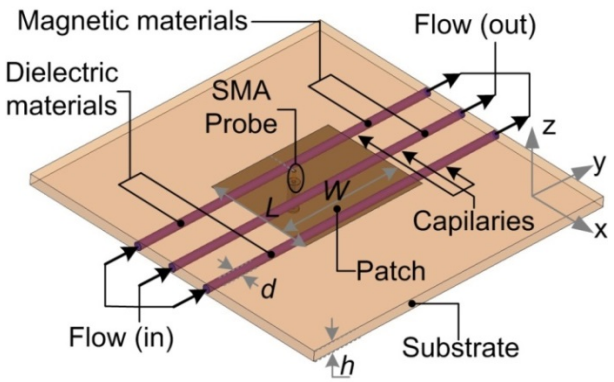

Figure 1. Microfluidic reconfigurable patch antenna. Fluids passing through the channels beneath the patch antenna can alter the resonant frequency and VSWR bandwidth.

Figure 2 shows a cross-section of a typical fluid channel used in the laboratory. The fluid is highly inhomogeneous and composed of electromagnetically functionalized colloidal dispersions (EFCDs) mixed in with a background liquid. If there is a high contrast between the electrical properties of these inclusions and the liquid, there is a change in the fluid's net effective electromagnetic properties according to a "mixing rule." In general, the mixing rule is dependent on the shape of the inclusion as well as the volume fraction relative to the background liquid [3]. Thus, when these fluids are used in the channels of patch antenna in Figure 1, reconfiguration can be achieved by varying the inclusion types and volume fraction, which in turn vary the net effective electromagnetic properties [2].

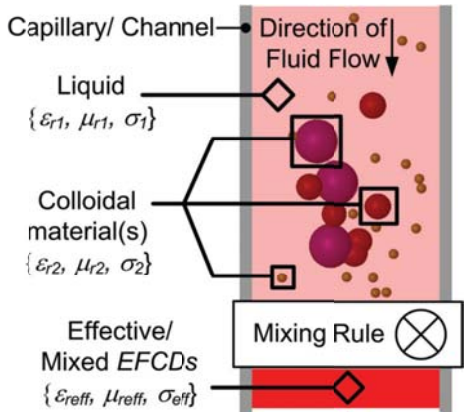

Figure 2. Electromagnetic Functionalized Colloidal Dispersions (EFCD). The colloidal materials are mixed in an electrically active liquid. The effective properties for this mixture are given by a mixing rule.

This thesis presents an analytical and numerical study of the effective medium theories for spherical colloidal dispersions. A review of electromagnetic theory and the classical mixing formulas is followed by an analysis of the interaction of two spherical dielectric inclusions in the presence of an applied time-harmonic electric field. A perturbation model is proposed that would adjust the Maxwell-Garnett theory for higher-order interactions. Finite-element simulations using COMSOL and Computer Simulation Technology Microwave Studio were performed to compute the effective permittivity and analyze the effects at high frequency.

CHAPTER II

THEORETICAL BACKGROUND

This chapter lays the theoretical foundations for our analytical and numerical studies of effective medium properties. The fundamental equations of electromagnetics are reviewed, and the definition of dielectric materials and permittivity are explained in detail. Additionally, the Maxwell-Garnett mixing rule is presented as the classical effective medium theory (EMT).

Review of the theory of electromagnetics and dielectric materials

In the field of electromagnetics engineering, the four most important partial differential equations are the time-harmonic Maxwell's equations [4]:

$$\nabla \times \vec{E} = -j\omega\mu\vec{H} \tag{1.1}$$

$$\nabla \times \vec{H} = j\omega\varepsilon\vec{E} + \vec{J} \tag{1.2}$$

$$\nabla \cdot \vec{D} = \rho \tag{1.3}$$

$$\nabla \cdot \vec{B} = 0 \tag{1.4}$$

Equations (1.1) and (1.2) are known as Ampere's Law and Faraday's Law, respectively; they describe the coupling between the electric field $\vec{E}$ and magnetic field $\vec{H}$ fields in a given system. Equations (1.3) and (1.4) are the Gauss's laws for electric and magnetic fields; they state that the point sources of electric fields are charges and that the point sources of magnetic fields do not exist. Because these four equations govern electromagnetic fields, all of the problems in electromagnetics can theoretically be solved by considering the equations with their proper boundary conditions [4].

Equations (1.3) and (1.4) contain the field quantities $\vec{D}$ and $\vec{B}$ in place of the standard field quantities because they describe the flux densities of the electric and magnetic fields. The constitutive equations give the relation between the two sets of field quantities:

$$\vec{D} = \varepsilon \vec{E} \tag{1.5}$$

$$\vec{B} = \mu \vec{H} \tag{1.6}$$

Here, the constants ε and μ represent the dielectric permittivity and magnetic permeability, which are material properties that measure how a given medium responds to an electromagnetic field. These two material quantities are often referred to by the relative quantities, ε_r and μ_r, whereby

$$\varepsilon = \varepsilon_r \varepsilon_0 \tag{1.7}$$

$$\mu = \mu_r \mu_0 \tag{1.8}$$

and ε_0 and μ_0 are the properties for a vacuum.

Physically, the dielectric permittivity (or relative permittivity) is a measure of the polarizability of a medium in the presence of an applied electric field. As an example, consider two parallel plates with a medium in between such as in Figure 3. An electrical potential difference applied across the two plates creates an electric field that passes through the sandwiched medium. The field induces small dipole moments in the bound charge of the medium; altogether, the dipole moments induce an electric field anti-parallel to the applied field. This “polarizing” effect is what defines a dielectric medium.

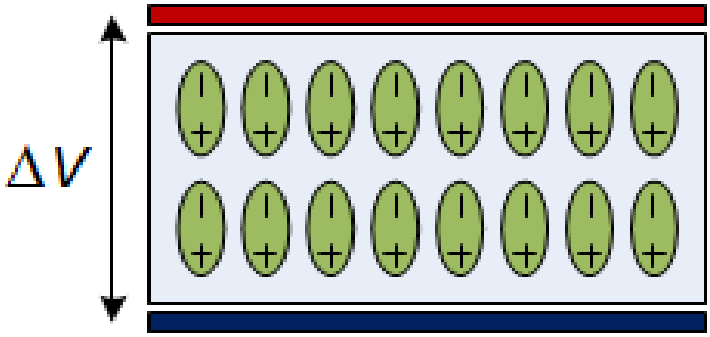

Figure 3. Two parallel plates sandwiching a dielectric medium. When the potential difference ΔV is applied across the plates, the internal bound and free charges align in the direction of the applied field.

For dielectric materials, the constitutive relation, Equation (1.5), has an additional term:

$$\vec{D} = \varepsilon \vec{E} + \vec{P} \tag{1.9}$$

where $\vec{P}$ is the average polarization vector (or average dipole moment), which is parallel to the direction of charge separation. In general, the relative dielectric permittivity of an anisotropic material is a rank-2 tensor whose elements depend on the direction of the applied field. This can become quite complicated, especially from a high-level, so the quantity "effective permittivity" or "net permittivity" is often used to describe materials.

Classical mixing theory

The topic of this thesis is the calculation and characterization of the effective dielectric constant ε_{eff} for mixtures. Consider a simple model of anisotropy—isotropic particles dispersed in an isotropic medium such as in Figure 2— and assume an electro quasi-static (EQS) regime, where the time varying components such as charge and current are approximately stationary [5]. The assumption requires that the size of the domain of interest is much smaller than one wavelength. Then, Maxwell's equations reduce to

$$\nabla \times \vec{E} = 0 \qquad (1.10)$$

$$\nabla \cdot \vec{D} = \rho \qquad (1.11)$$

Now, consider the effective medium problem for a mixture composed of a single type of spherical inclusion in an isotropic background medium. Using simple averaging arguments, the expression for the effective permittivity can be derived and would yield the well-known Maxwell-Garnett mixing rule [3]:

$$\varepsilon_{eff} = \varepsilon_e + 3f\varepsilon_e \frac{\varepsilon_i - \varepsilon_e}{\varepsilon_i + 2\varepsilon_e - f\left(\varepsilon_i - \varepsilon_e\right)} \qquad (1.12)$$

Here, ε_e is the background medium permittivity; ε_i is the inclusion permittivity; and f is the volume fraction of the inclusion. The validity of this averaging approach depends completely on the assumption that the individual spherical inclusions do not interact with each other; when the volume fraction is low—i.e. the particles are sufficiently spaced—this assumption holds [6]. Yet, both experimental and computational work has shown that the theory breaks down as the volume fraction of the inclusions increases towards the theoretical maximum.

Given the assumptions, Equation (1.12) can be extended to double-layered spherical inclusions. For reference purposes, the Maxwell-Garnett rule in this case is [3]

$$\frac{\varepsilon_{eff} - \varepsilon_e}{\varepsilon_{eff} + 2\varepsilon_e} = f \frac{\left(\varepsilon_1 - \varepsilon_e\right)\left(\varepsilon_2 + 2\varepsilon_1\right) + \frac{r_2^3}{r_1^3}\left(\varepsilon_2 - \varepsilon_1\right)\left(\varepsilon_e + 2\varepsilon_1\right)}{\left(\varepsilon_1 + 2\varepsilon_e\right)\left(\varepsilon_2 + 2\varepsilon_1\right) + 2\frac{r_2^3}{r_1^3}\left(\varepsilon_2 - \varepsilon_1\right)\left(\varepsilon_1 - \varepsilon_e\right)} \qquad (1.13)$$

Many other extensions such as multiphase and non-spherical shapes have also been generated ad nauseam and are readily available in the mixing theory literature [3].

CHAPTER III

ANALYTICAL APPROACH

This chapter discusses the analytical approach to develop an effective permittivity formula that accounts for the multi-particle interactions. In the laboratory applications, the standard dielectric mixture are high dielectric Barium Strontium Titanate (BSTO) spherical inclusions dispersed in a low dielectric silicone oil or electrically active fluid such as Flourinert FC-70. The oil or inert fluid coats the outside of the spherical BSTO particles, forming a conductive shell. A conductive (lossy) dielectric double-layer models the shell.

Single layered dielectric inclusions

Consider a layered dielectric sphere in the presence of an applied AC electric field such as in Figure 4.

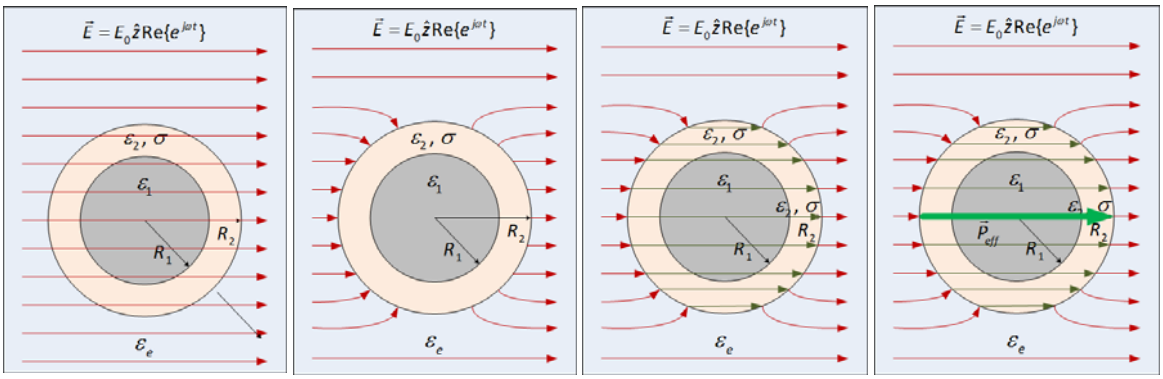

Figure 4. A layered dielectric sphere in the presence of a z -directed applied AC electric field. The outer layer is assumed to be lossy. As the electric field passes through the dielectric particle, a uniform internal field is induced, parallel to the direction of the primary field. Moreover, a net polarization is induced inside the layers.

The potential distribution of this problem is by Equations (2.1) - (2.3) where the three regions are designated by three distinct subscripts [7].

$$\phi_{EXT}(r,\theta)=\left(-E_0 r+\frac{A}{r^2}\right)\cos\theta, \qquad r>R_2 \tag{2.1}$$

$$\phi_2(r,\theta)=\left(-Br+\frac{C}{r^2}\right)\cos\theta, \qquad R_2>r>R_1 \tag{2.2}$$

$$\phi_1(r,\theta)=-Dr\cos\theta, \qquad R_1>r \tag{2.3}$$

For simplicity, we work in the phasor domain so that the factor $\mathrm{Re}\left\{e^{j\omega t}\right\}$ is absorbed into the constant E_0. The constants, A, B, C, and D, are given by [7]

$$A=\frac{\varepsilon_1'-\varepsilon_e}{\varepsilon_1'+2\varepsilon_e}R_2{}^3E_0 \tag{2.4}$$

$$B=-\frac{3\varepsilon_e\left(\frac{R_2}{R_1}\right)^3}{\left(\varepsilon_1'+2\varepsilon_e\right)\left(\left(\frac{R_2}{R_1}\right)^3-K\right)}E_0 \tag{2.5}$$

$$C=-\frac{3\varepsilon_e K R_2{}^3}{\left(\varepsilon_1'+2\varepsilon_e\right)\left(\left(\frac{R_2}{R_1}\right)^3-K\right)}E_0 \tag{2.6}$$

$$D=-\frac{3\varepsilon_e(1-K)\left(\frac{R_2}{R_1}\right)^3}{\left(\varepsilon_1'+2\varepsilon_e\right)\left(\left(\frac{R_2}{R_1}\right)^3-K\right)}E_0 \tag{2.7}$$

Here, ε_1' is the effective permittivity of the double-layered particle, and K is the Clausius-Mossotti factor. They are used instead of explicitly referring to the three different permittivities to ensure that the mathematical expressions remain manageable [7]. Their values are given by

$$\varepsilon_1' = \varepsilon_2 \left(\frac{\left(\frac{R_2}{R_1}\right)^3 + 2\frac{\varepsilon_1 - \varepsilon_2}{\varepsilon_1 + 2\varepsilon_2}}{\left(\frac{R_2}{R_1}\right)^3 - 2\frac{\varepsilon_1 - \varepsilon_2}{\varepsilon_1 + 2\varepsilon_2}} \right) \tag{2.8}$$

$$K = \frac{\varepsilon_1' - \varepsilon_e}{\varepsilon_1' + 2\varepsilon_e} \tag{2.9}$$

Additionally, the permittivities can be complex valued, $\varepsilon_n = \varepsilon_{r_n} - j\frac{\sigma_n}{\omega\varepsilon_0}$. From Equations (2.1) through (2.3), the corresponding electric field is simply computed as $E = -\nabla\phi(r,\theta)$, where the gradient is taken in cylindrical coordinates.

$$\vec{E}_{EXT}(r,\theta) = \left(E_0\cos\theta\hat{r} - E_0\sin\theta\hat{\theta}\right) + \left(\frac{2A}{r^3}\cos\theta\hat{r} + \frac{A}{r^3}\sin\theta\hat{\theta}\right) \tag{2.10}$$

$$\vec{E}_2(r,\theta) = \left(B\cos\theta\hat{r} - B\sin\theta\hat{\theta}\right) + \left(\frac{2C}{r^3}\cos\theta\hat{r} + \frac{C}{r^3}\sin\theta\hat{\theta}\right) \tag{2.11}$$

$$\vec{E}_1(r,\theta) = D\cos\theta\hat{r} - D\sin\theta\hat{\theta} \tag{2.12}$$

The electric field expressions above are written in a form that separates the $\frac{1}{r^3}$ dependency in the various terms. Examining the expression for the external field, we can see that the field is given by the superposition of the applied field and the perturbation in the presence of the layered dielectric sphere. Mathematically, we can then write

$$\vec{E}_{EXT}(r,\theta) = \vec{E}_{APP}(r,\theta) + \vec{E}_{PERTURBED}(r,\theta) \tag{2.13}$$

As one gets far enough away from the layered sphere, the field appears uniform. In the rest of this thesis, an approximation is made that when $r > 10R_2$, the field can be considered uniform because the perturbing field will have been reduced by 10^{-3}, or -3 dB.

Two layered dielectric inclusions

Now consider a system of two layered dielectric particles, spaced a distance R_d from each other (see Figure 5).

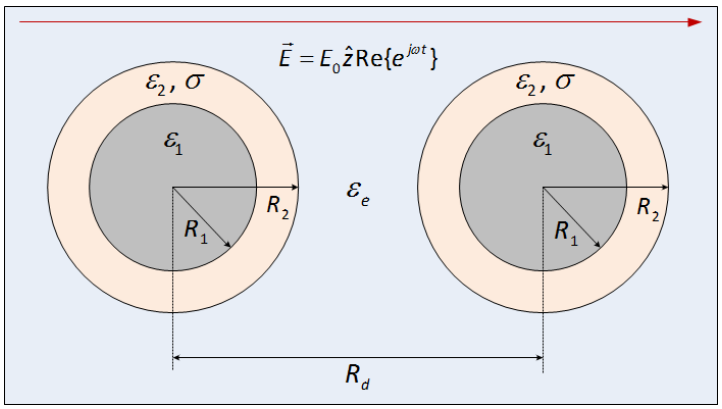

Figure 5. Two layered dielectric spheres separated by a distance R_d **.**

Just as before, the applied electric field induces a polarization inside each particle. Physically, this causes the free charge from the lossy surface to reorient along the edges, such as in Figure 6. As R_d gets smaller, the particles become closer, which models an increased volume fraction. This charge separation then induces a second order interaction between the two particles, modeled as an induced polarization anti-parallel to the direction of the applied field.

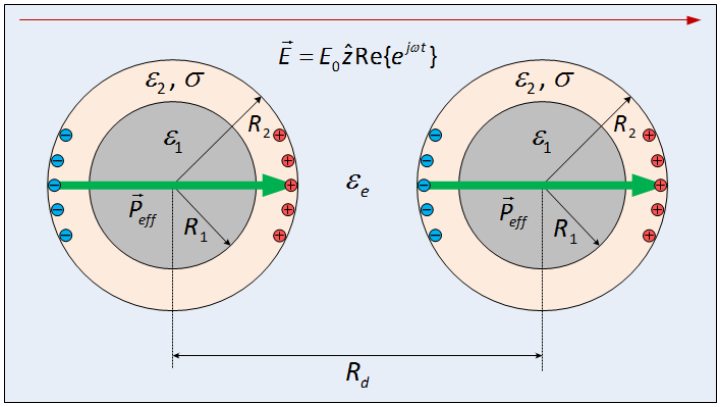

Figure 6. Induced polarization on both spheres. A charge separation is formed on the surface and distributes itself in the direction of the induced polarization.

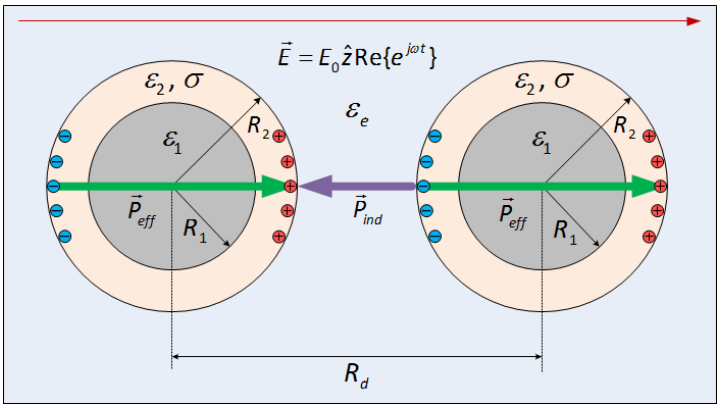

Figure 7. Polarization induced by the charge separation on surface of the spheres.

Mathematically, suppose that he first particle is located at the center of a cylindrical coordinate system; the second particle would then be a vertical displacement R_d away. Figure 8 displays the geometrical setup. Then, the relation between the primed and unprimed coordinate systems is given by

$$r' = \sqrt{r^2 + {R_d}^2 - 2rR_d \cos\theta} \tag{2.14}$$

$$\theta' = \pi - \cos^{-1}\left(\frac{2R_d + r\cos\theta}{2\sqrt{r^2 + {R_d}^2 - 2rR_d\cos\theta}}\right) \tag{2.15}$$

The external potential generated by shifted dielectric sphere is

$$\phi_{EXT}(r,\theta) = \left(-E_0\sqrt{r^2 + {R_d}^2 - 2rR_d\cos\theta} + \frac{A}{r^2 + {R_d}^2 - 2rR_d\cos\theta}\right)\cos\theta' \tag{2.16}$$

Now, recalling the trigonometric identity relating a shifted cosine term, the term $\cos\theta'$ becomes

$$\cos\theta' = \cos\left(\pi - \cos^{-1}\left(\frac{2R_d + r\cos\theta}{2\sqrt{r^2 + {R_d}^2 - 2rR_d\cos\theta}}\right)\right) = -\frac{2R_d + r\cos\theta}{2\sqrt{r^2 + {R_d}^2 - 2rR_d\cos\theta}} \tag{2.17}$$

To evaluate the external field, one can either evaluate the gradient on the shifted external potential or substitute the coordinate transformations. The final expression for the external field of the shifted dielectric is a complex expression in terms of the original spherical coordinates.

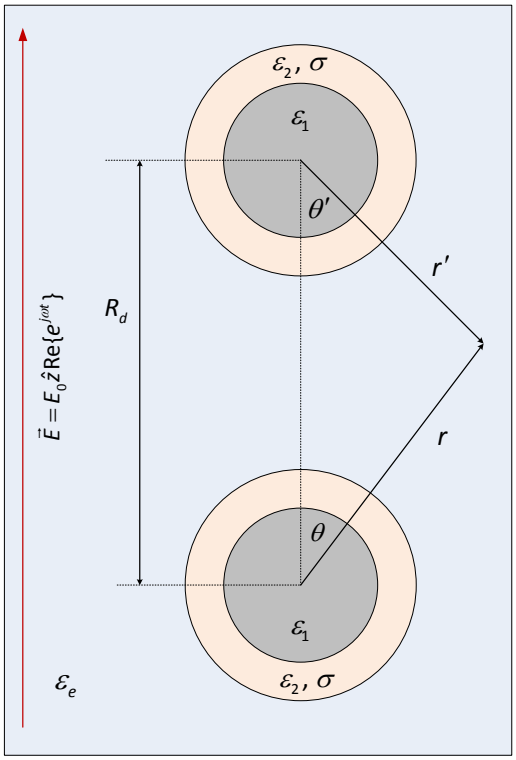

Figure 8. Geometry of the shifted second particle.

If the distance between these particles is greater than the limit defined in the previous subsection, the total external electric field appears uniform, and the interaction between the particles is negligible.

Field perturbation analysis

Using the two-particle framework developed in the previous subsection, consider the problem of the two dielectric spheres as they approach one another. This physically occurs in the fluid mixture as the volume fraction approaches the percolation threshold, and the interactions between each of the particles are no longer negligible. Using the radial limit defined in the prior subsection, let the electric field outside of a given particle be given by

$$\vec{E}_{EXT}\left(r,\theta\right)=\begin{cases}\vec{E}_{EXT}^{EXT}\left(r,\theta\right), & r>10r_p\\ \vec{E}_{EXT}^{INT}\left(r,\theta\right), & r<10r_p\end{cases}=\begin{cases}\vec{E}_{UNIFORM}, & r>10r_p\\ \vec{E}_{EXT}^{INT}\left(r,\theta\right), & r<10r_p\end{cases} \tag{2.18}$$

where the field is now divided into two regions, inside and outside of the radial limit.

If the two dielectric spheres are far enough apart, the field seen at the center point between the particles is approximately just the uniformly applied field. Now consider the situation when the two particles are close enough such that the center point between the two fields is inside of the radial limit of both particles. In this overlapping region, the electric field is a positive perturbation on the normal field inside the radial limit. This perturbed interaction is a model for the two-particle interaction as the volume fraction of the spherical inclusions increases to and past the percolation threshold.

With some physical intuition, this perturbation can be modeled as the inclusion of a high dielectric prolate spheroid between the particles. As the volume fraction increases, there is deviation from the Maxwell-Garnett theory, and the measured effective permittivity is greater than the predicted value. Currently, this model is not completely resolved. However, the technique would be to analyze the perturbation back-calculate what the dimensions and permittivity of the induced prolate spheroid should be that would resemble the deviation from Maxwell-Garnett. Then, a new effective medium formula can be derived using a standard multiphase mixture analysis.

CHAPTER IV

NUMERICAL SIMULATIONS

This chapter discusses the finite-element simulations performed to compute the effective permittivity of various particle geometries and compare them with the classical Maxwell-Garnett effective medium theories. Two different finite-element programs were used: COMSOL Multiphysics and Computer Simulation Technology - Microwave Studio (CST-MWS). In COMSOL, the setup consisted of modeling a periodic unit-cell and applying a bias voltage between two the two faces; the volume-average electric field and electric displacement fields were computed to solve for the effective permittivity. This method is adopted from Lee *et al*. [8] During the analysis, COMSOL failed at lower-frequencies and yielded some numerical inaccuracies, so CST-MWS was chosen as a secondary benchmark. Following the material measurements technique used in the laboratory, transverse electric (TE) plane-wave incidence on the periodic unit cell was simulated using a Floquet analysis, and the effective permittivity was extracted from the computed de-embedded S_{21} parameter.

To model a large distribution of colloidal dispersions, a periodic unit cell was analyzed for various known crystal lattice configurations. These consist of the simple-cubic, body-centered cubic, and face-centered cubic lattices. The domain is then the particles aligned according to one of the distributions and a background fluid. Periodic boundary conditions applied on four adjacent faces simulate an infinite extension in two dimensions while an applied AC voltage or incident wave excites the structure. Figures 8-10 show the various distributions as they were in COMSOL. The CST-MWS model was geometrically the same.

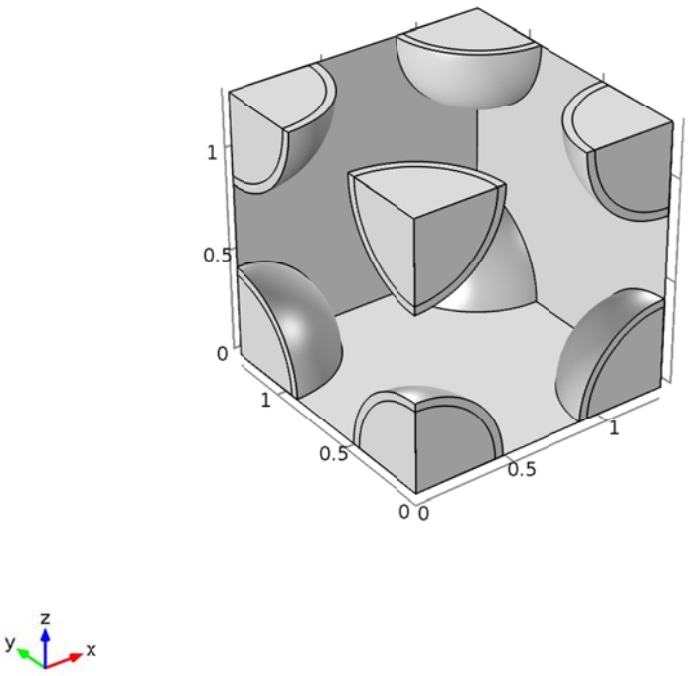

Figure 9. Simple cubic distribution with outer shell.

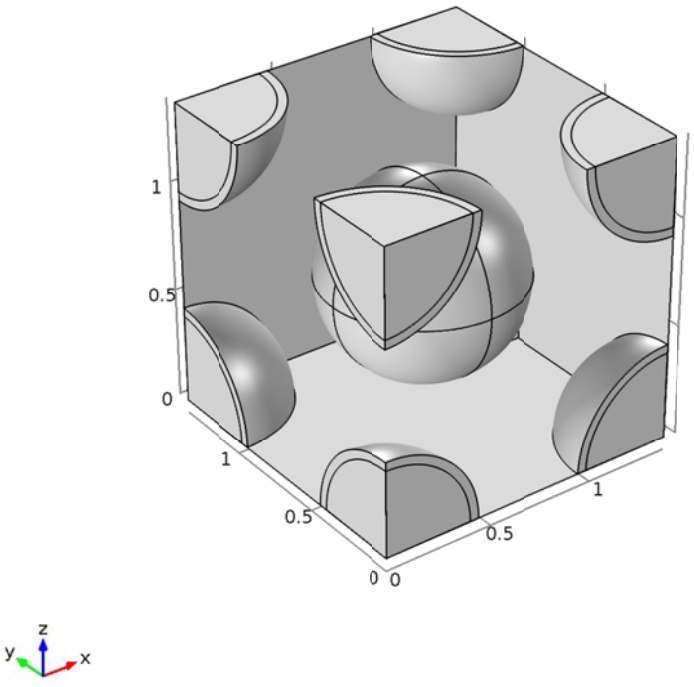

Figure 10. Body-centered cubic (BCC) distribution with outer shell.

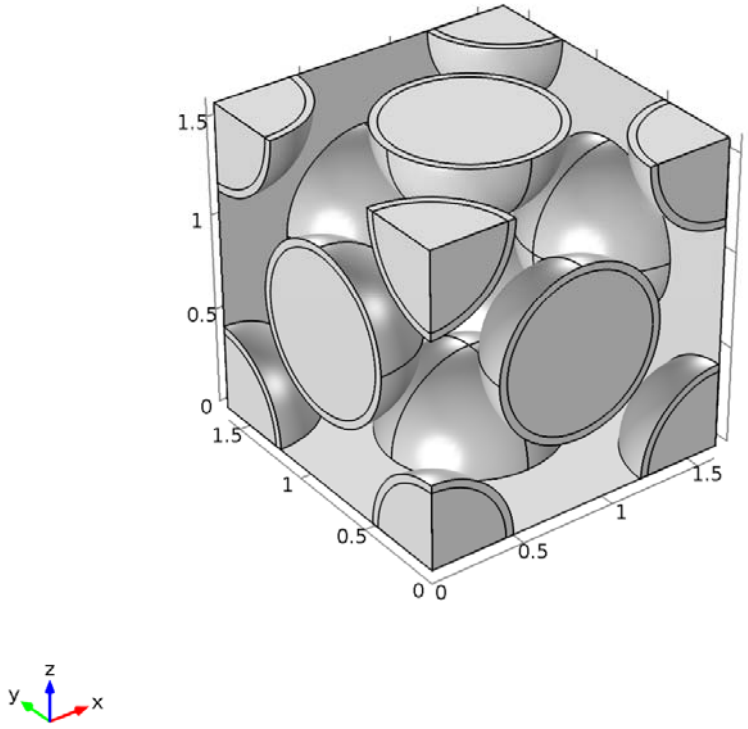

Figure 11. Face-centered cubic (FCC) distribution with outer shell.

COMSOL simulation setup and governing equations

In the COMSOL simulation, an alternating current (AC) voltage is applied across two opposite faces. This simulates an electric current passing through the particles. The governing equations are then simply current continuity, current conservation, and electric potential equations:

$$\nabla \cdot \vec{J} = Q_j \tag{2.19}$$

$$\vec{J} = \left(\sigma + j\omega\grave{o}_0\grave{o}_r\right)\vec{E} + \vec{J}_e \tag{2.20}$$

$$\vec{E} = -\nabla V \tag{2.21}$$

The effective permittivity of a single unit cell can be extracted from the basic constitutive relation Equation (1.5). In order for this method to be valid, all of the materials are assumed to be linear and isotropic. In matrix form, the constitutive relation is

$$\begin{pmatrix} D_x \\ D_y \\ D_z \end{pmatrix} = \begin{pmatrix} \varepsilon_{xx} & \varepsilon_{xy} & \varepsilon_{xz} \\ \varepsilon_{yx} & \varepsilon_{yy} & \varepsilon_{yz} \\ \varepsilon_{zx} & \varepsilon_{zy} & \varepsilon_{zz} \end{pmatrix} \begin{pmatrix} E_x \\ E_y \\ E_z \end{pmatrix} \tag{2.22}$$

The assumption of isotropy and linearity leads to a symmetric permittivity matrix. Furthermore, since the field is applied in a single direction, the exciting vector field $\vec{E}$ can be approximated by

$$\vec{E} \approx \begin{pmatrix} E_x \\ 0 \\ 0 \end{pmatrix} \tag{2.23}$$

This simplifies Equation (2.22) yielding

$$\begin{pmatrix} D_x \\ D_y \\ D_z \end{pmatrix} \approx \begin{pmatrix} \varepsilon_{xx} \\ \varepsilon_{yx} \\ \varepsilon_{zx} \end{pmatrix} \begin{pmatrix} E_x \\ 0 \\ 0 \end{pmatrix} \tag{2.24}$$

Equation (2.24) is dependent on the location within the discretized unit cell. Taking a volumetric average of the four field quantities in Equation (2.24) extracts the volumetric average permittivity components.

$$\begin{pmatrix} \langle D_x \rangle \\ \langle D_y \rangle \\ \langle D_z \rangle \end{pmatrix} \approx \begin{pmatrix} \varepsilon_{xx} \\ \varepsilon_{yx} \\ \varepsilon_{zx} \end{pmatrix} \begin{pmatrix} \langle E_x \rangle \\ 0 \\ 0 \end{pmatrix} \tag{2.25}$$

Since the particle distribution consists of uniformly shaped spherical inclusions, the total effective permittivity has only one non-zero component, ε_{xx}. The analysis above assumes an excitation in the x direction. A similar setup with excitations in the y and z directions results

in the other diagonal components of the permittivity matrix, ε_{yy} and ε_{zz}. Finally, by symmetry arguments,

$$\varepsilon_{xx} = \varepsilon_{yy} = \varepsilon_{zz} \tag{2.26}$$

up to numerical accuracy of the discretization.

CST Microwave Studio setup

In contrast to the volumetric averaging technique in COMSOL, the effective property simulation with CST-MWS is based on the material measurements technique used in the laboratory **[9]**. An unknown material is placed between two known materials. A plane-wave is excited at the first boundary, which transmits and reflects through the material. Floquet ports with only the TE_{00} modes model the incident plane wave. The frequency domain solver is used. CST-MWS can extract the scattering parameters of the system. The remaining task is to extract the material permittivity from the parameters.

Computing Material Properties from Scattering Parameters

Consider a three-part scattering problem modeled as a two-port transmission line network, such as in Figure 12. An electromagnetic plane wave incident to the material under test (MUT) reflects and transmits through both boundaries of the medium. The two-port scattering parameters capture the physics of the bouncing reflections and transmissions on both interfaces.

The reflection coefficient between the first outer-MUT interfaces is

$$\Gamma_1 = \frac{Z_s - Z}{Z_s + Z} = \frac{\bar{Z}_s - \bar{Z}}{\bar{Z}_s + \bar{Z}} = \frac{\sqrt{\frac{\mu_r}{\varepsilon_r}} - \sqrt{\frac{\mu_{r1}}{\varepsilon_{r1}}}}{\sqrt{\frac{\mu_r}{\varepsilon_r}} + \sqrt{\frac{\mu_{r1}}{\varepsilon_{r1}}}} \tag{2.27}$$

where $\bar{Z}_s$ and $\bar{Z}$ are the sample and boundary impedances, respectively, normalized to the impedance of air, η_0.

$$\bar{Z}_s = \sqrt{\frac{\mu_r}{\varepsilon_r}} \tag{2.28}$$

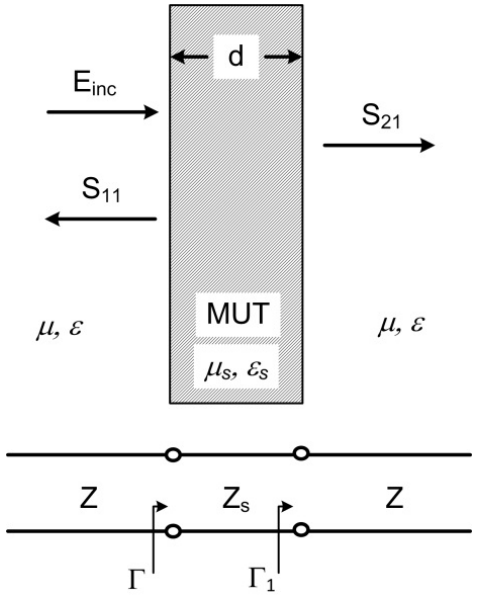

Figure 12. **Two-port network model to measure material properties.**

$$\bar{Z} = \sqrt{\frac{\mu_{r_1}}{\varepsilon_{r_1}}} \tag{2.29}$$

In general, the material properties ε and μ are complex quantities. For the purposes of this analysis, the outer material is assumed to be lossless. The reflection coefficient at the second MUT-outer boundary is $\Gamma_2 = -\Gamma_1$. The transmission coefficient through the MUT is

$$T = e^{-j\beta_s d} = e^{-j\beta_0\sqrt{\varepsilon_r\mu_r}d} = e^{-j\frac{2\pi}{\lambda_0}\sqrt{\varepsilon_r\mu_r}d} \tag{2.30}$$

The end goal is to drive an expression for the scattering parameters in terms of the material properties. To this end, this analysis has been performed and the end result is given by [9]

$$S_{21} = \frac{\left(1-\Gamma^2\right)T}{1-\left(\Gamma T\right)^2} = \frac{e^{-j\frac{2\pi}{\lambda_0}\sqrt{\varepsilon_r\mu_r}d}\left(1-\left(\frac{\sqrt{\frac{\mu_r}{\varepsilon_r}}-\sqrt{\frac{\mu_{r1}}{\varepsilon_{r1}}}}{\sqrt{\frac{\mu_r}{\varepsilon_r}}+\sqrt{\frac{\mu_{r1}}{\varepsilon_{r1}}}}\right)^2\right)}{1-\left(e^{-j\frac{2\pi}{\lambda_0}\sqrt{\varepsilon_r\mu_r}d}\left(\frac{\sqrt{\frac{\mu_r}{\varepsilon_r}}-\sqrt{\frac{\mu_{r1}}{\varepsilon_{r1}}}}{\sqrt{\frac{\mu_r}{\varepsilon_r}}+\sqrt{\frac{\mu_{r1}}{\varepsilon_{r1}}}}\right)\right)^2} \tag{2.31}$$

For dielectric materials, the relative magnetic permeabilities are equal to 1. The final equation is then

$$S_{21}\left(\varepsilon_r\right) = \frac{e^{-j\frac{2\pi}{\lambda_0}\sqrt{\varepsilon_r}d}\left(1-\left(\frac{\sqrt{\frac{1}{\varepsilon_r}}-\sqrt{\frac{1}{\varepsilon_{r1}}}}{\sqrt{\frac{1}{\varepsilon_r}}+\sqrt{\frac{1}{\varepsilon_{r1}}}}\right)^2\right)}{1-e^{-j2\frac{2\pi}{\lambda_0}\sqrt{\varepsilon_r}d}\left(\frac{\sqrt{\frac{1}{\varepsilon_r}}-\sqrt{\frac{1}{\varepsilon_{r1}}}}{\sqrt{\frac{1}{\varepsilon_r}}+\sqrt{\frac{1}{\varepsilon_{r1}}}}\right)^2} \tag{2.32}$$

To extract the permittivity from the simulated S_{21} parameter, one can solve the system

$$S_{21}^P\left(\varepsilon_r\right) - S_{21}^C = 0 \tag{2.33}$$

where $S_{21}^p\left(\varepsilon_r\right)$ is given by Equation (2.32) and S_{21}^C is the computed value from the CST Microwave Studio simulation.

Results from COMSOL simulations

In both configurations, various simulations were run for the BCC, FCC, and single particle distributions. The inclusions consisted of either a single or double layer dielectric, where the double layer had a lossy conductivity. In both simulations, the background fluid was chosen to be a silicone oil with a dielectric constant of 2.1. In the CST-MWS case, a small conductive loss was included for the silicone oil. Parametric sweeps over particle radii, particle permittivity, and frequency were performed.

In all of the COMSOL cases, the field solutions were plotted over the special domain. In general, they all resemble Figure 13, varying only slightly depending on the chosen particle distribution.

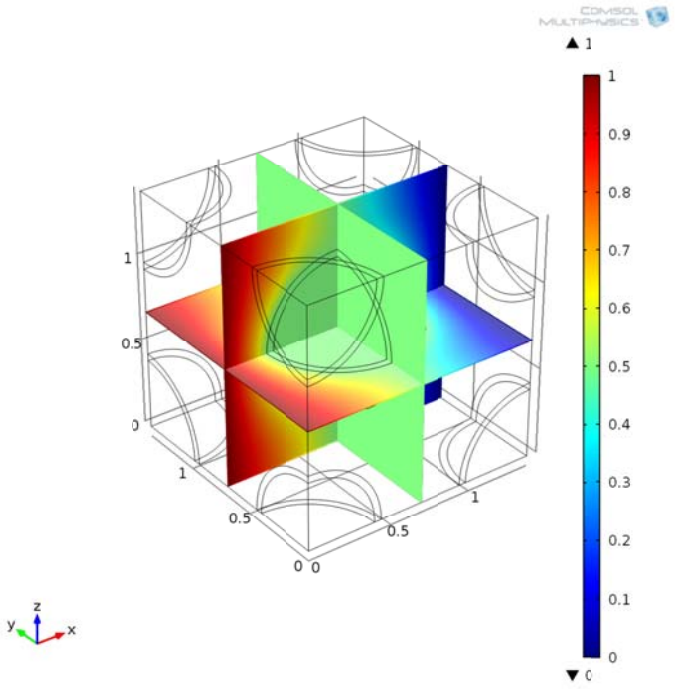

Figure 13. Potential distribution across a BCC particle distribution.

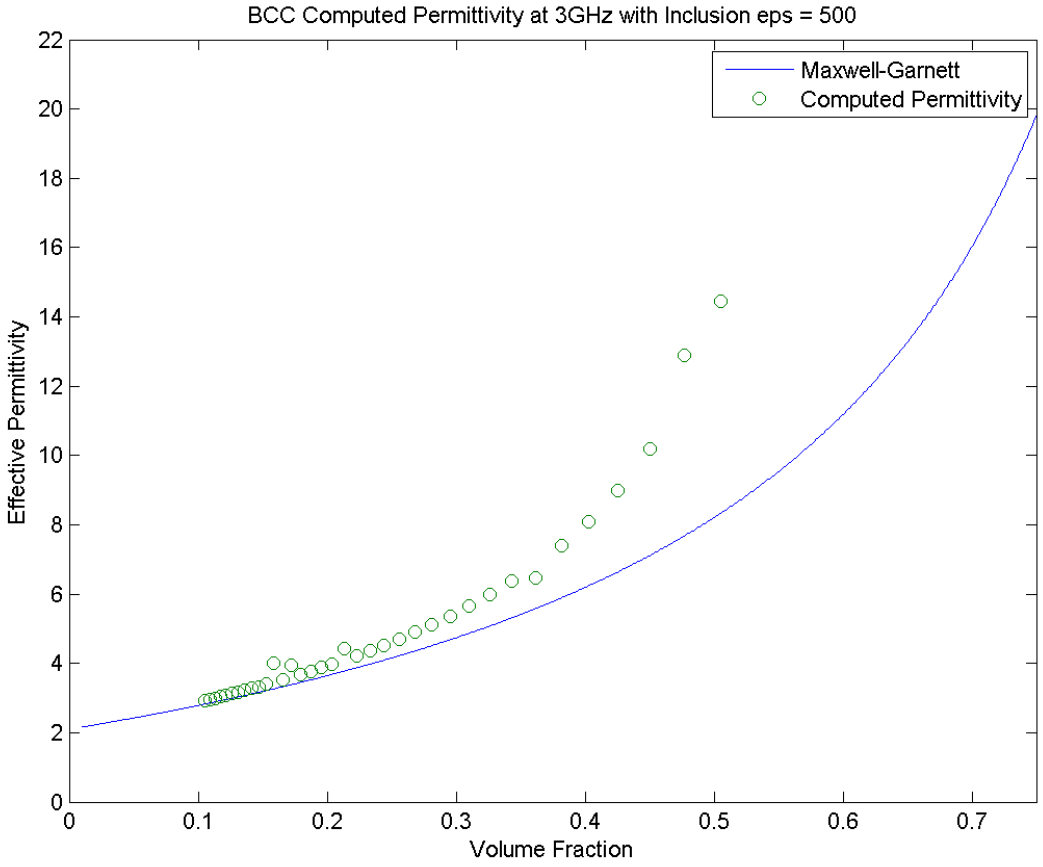

Figure 14. BCC COMSOL Computed Permittivity at 3GHz and $\varepsilon_r = 500$.

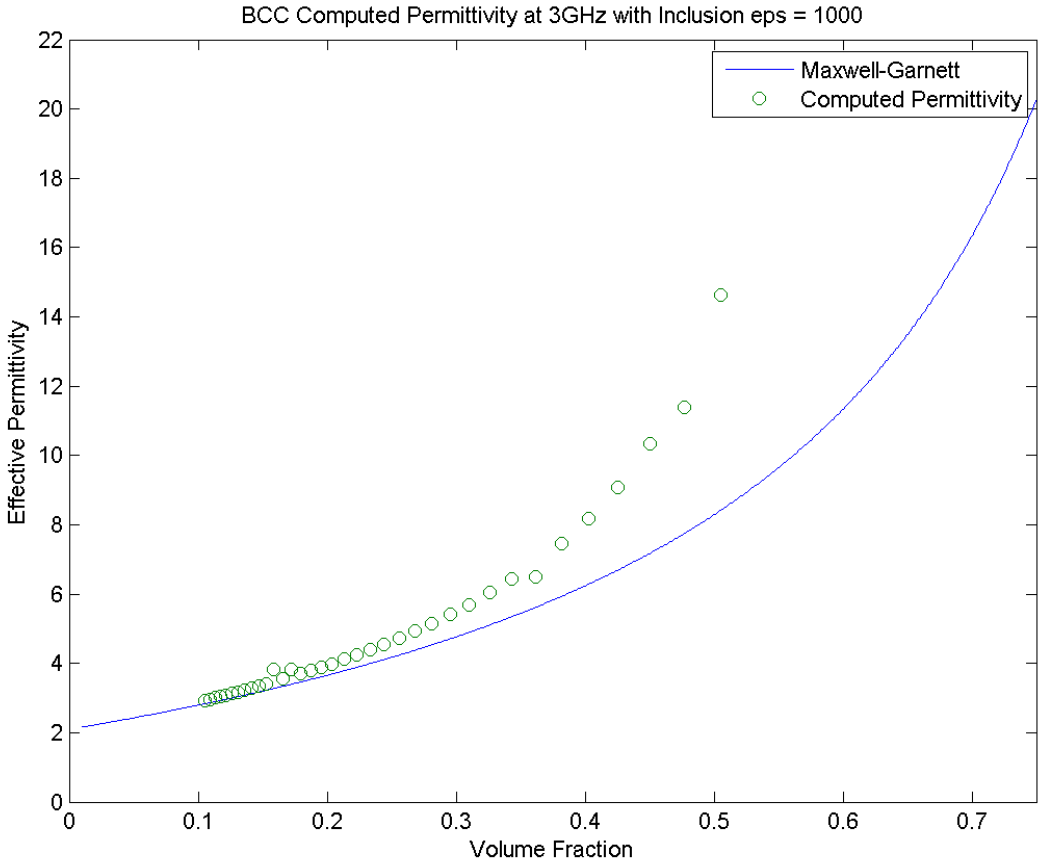

Figure 15. BCC COMSOL Computed Permittivity at 3GHz and $\varepsilon_r = 1000$.

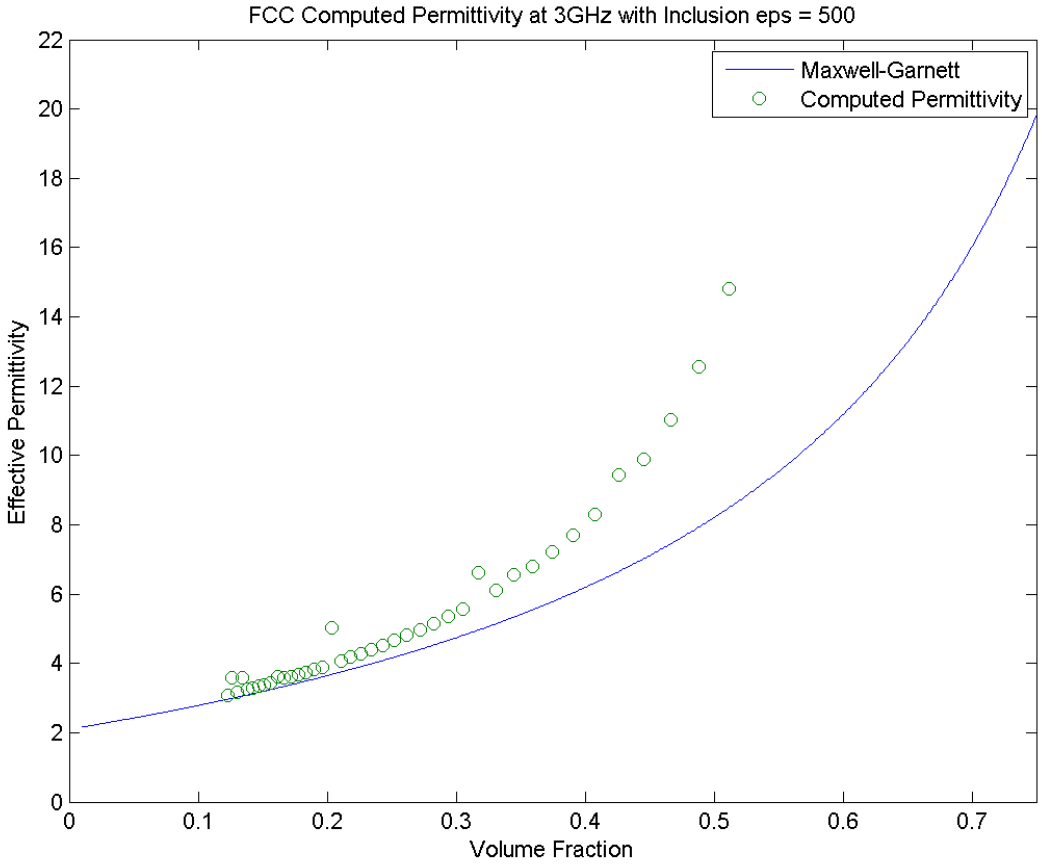

Figure 16. FCC COMSOL Computed Permittivity at 3GHz and $\varepsilon_r = 500$.

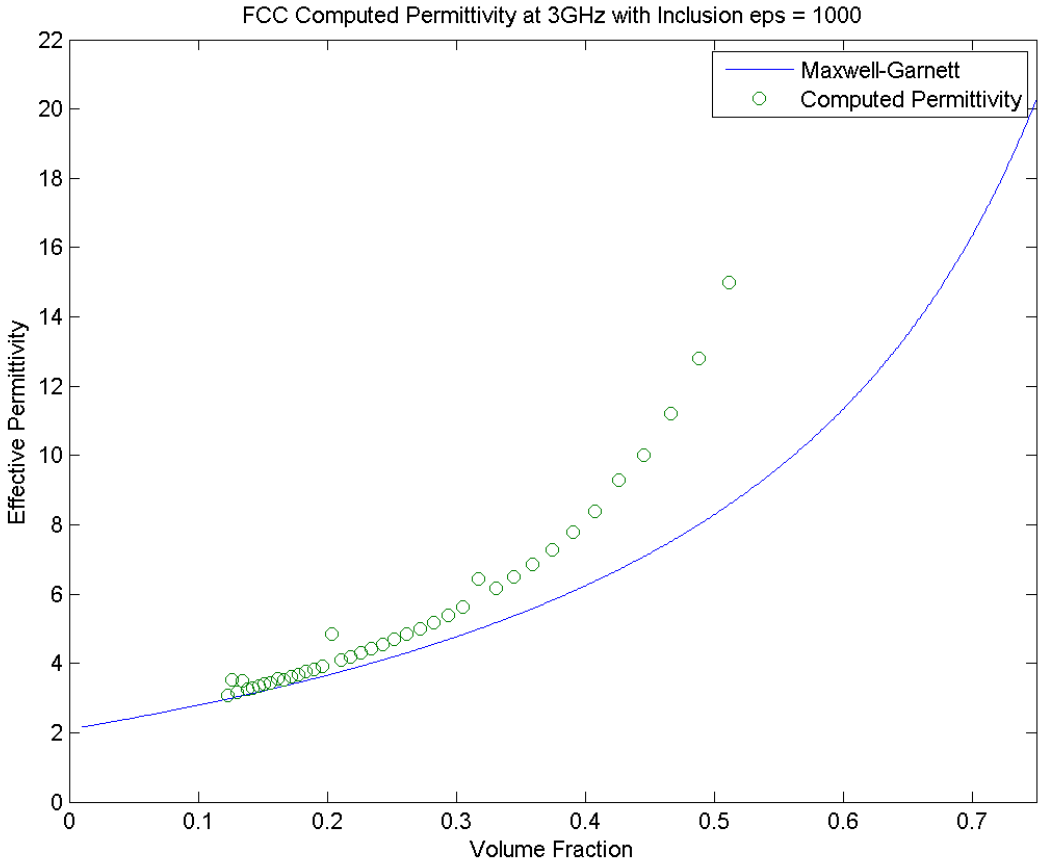

Figure 17. FCC COMSOL Computed Permittivity at 3GHz and $\varepsilon_r = 1000$.

Figures 14-17 above show the computed results from the COMSOL simulations at 3GHz for two different particle permittivities. Clearly, a deviation from Maxwell-Garnett is seen as the volume fraction increases above 30%.

Currently, the simulation results from CST-MWS are still being analyzed, so they are not available.

CHAPTER V

CONCLUSIONS AND FUTURE WORK

The analytical model presented in this thesis provides insight into modeling the interactions between multiple particles in a mixed medium. Modeling of the prolate inclusions will modify the standard Maxwell-Garnett formulas and likely account for the increase in effective permittivity seen by the numerical simulations. COMSOL Multiphysics proved to be problematic at handling low-frequency calculations, but at 3GHz, the results clearly indicate a deviation from Maxwell-Garnett.

Future work includes finishing the perturbation analysis on the two-particle inclusion to compute a new effective medium formula. Additionally, further investigation into how COMSOL numerically solve the partial differential equations will be performed to verify the validity of the software package. Further, the analysis on the CST-MWS studio will be completed to examine the computed effective permittivity with this method. Laboratory analysis using the material measurements system will be undertaken to serve as a final comparison between the classical theory, new model, and numerical results.

REFERENCES

[1] David M. Pozar, *Microwave Engineering*, 4th ed. Hoboken, New Jersey: John Wiley & Sons, 2012.

[2] Sean Goldberger et al., "Frequency Reconfiguration of a Small Array Enabled by Functionalized Dispersions of Colloidal Material," in *23rd Annual Conference on Small Satelites*, Logan, UT, 2009.

[3] Ari Sihvola, *Electromagnetic Mixing Formulas*, 1st ed. London, United Kingdom: The Institution of Electrical Engineers, 1999.

[4] Julias A. Stratton, *Electromagnetic Theory*. Hoboken, New Jersey: John Wiley & Sons, 2007.

[5] Roger F. Harrington, *Time-Harmonic Electromagnetic Fields*. Hoboken, New Jersey: John Wiley & Sons, 2001.

[6] A. Alexopoulos, "Effective-medium theory of surfaces and metasurfaces containing two-dimensional binary inclusions," *Physical Review E*, vol. 81, no. 046607, pp. 1-12, April 2010.

[7] Thomas B. Jones, *Electromechanics of Particles*, 1st ed. Cambridge, United Kingdom: Cambridge University Press, 1995.

[8] J., J. Lee, J. G. Boyd, and D. C. Lagoudas, "Effective Properties of Three-Phase Electro-Magneto-Elastic Composites," *International Journal of Engineering Science*, vol. 43, pp. 790-825, 2005.

[9] A. M. Nicholson and G. F. Ross, "Measurement of the Intrinsic Properties of Materials by Time-Domain Techniques," *IEEE Transactions on Instrumentation and Measurement*, vol. 19, no. 4, pp. 377-382, November 1970.

[10] Franklin Drummond, "Finite Element Studies of Colloidal Mixtures Influenced by Electric Fields," *Texas A&M University*, August 2011.